PPARα controls the intracellular coenzyme A concentration via regulation of *PANK1α* gene expression[1]

Gayathri Ramaswamy,[*,§] Mohammad A. Karim,[2,*] K. Gopal Murti,[†,] and Suzanne Jackowski[3,*,§]**

Protein Science Division,* Department of Infectious Diseases, and Scientific Imaging Shared Resource,† St. Jude Children's Research Hospital, Memphis, TN 38105-2794; and the Departments of Molecular Sciences§ and Pathology,** University of Tennessee Health Science Center, Memphis, TN 38163

Abstract **Pantothenate kinase (PanK) is thought to catalyze the first rate-limiting step in CoA biosynthesis. The full-length cDNA encoding the human PanK1α protein was isolated, and the complete human *PANK1* gene structure was determined. Bezafibrate (BF), a hypolipidemic drug and a peroxisome proliferator activator receptor-α (PPARα) agonist, specifically increased *hPANK1α* mRNA expression in human hepatoblastoma (HepG2) cells as a function of time and dose of the drug, compared with *hPANK1β*, *hPANK2*, and *hPANK3*, which did not significantly increase. Four putative PPARα response elements were identified in the *PANK1α* promoter, and BF stimulated *hPANK1α* promoter activity but did not alter the mRNA half-life. Increased *hPANK1α* mRNA resulted in higher hPanK1 protein, localized in the cytoplasm, and elevated PanK enzyme activity. The enhanced *hPANK1α* gene expression translated into increased activity of the CoA biosynthetic pathway and established a higher steady-state CoA level in HepG2 cells. These data are consistent with a key role for PanK1α in the control of cellular CoA content and point to the PPARα transcription factor as a major factor governing hepatic CoA levels by specific modulation of *PANK1α* gene expression.**—Ramaswamy, G., M. A. Karim, K. G. Murti, and S. Jackowski. **PPARα controls the intracellular coenzyme A concentration via regulation of *PANK1α* gene expression. *J. Lipid Res.* 2004.** 45: **17–31.**

Supplementary key words pantothenate • pantothenate kinase • peroxisome proliferator activator receptor-α • fatty acid β-oxidation • liver

Pantothenate (Pan) is a B complex vitamin (B_5) and is a nutritional requirement in mammals. Pan is the precursor for the biosynthesis of CoA, the predominant acyl group carrier in cells. Acyl moieties are attached to the terminal sulfhydryl of CoA, and these compounds participate in over 100 different reactions in intermediary metabolism (1–4). Short-chain CoA thioesters, such as acetyl-CoA or succinyl-CoA, are the most abundant components of the CoA pool (5) and are important intermediates in the tricarboxylic acid cycle, which coordinates carbon utilization and oxidative energy production. CoA is also an essential cofactor in long-chain fatty acid metabolism. CoA transfers fatty acids to and from the mitochondrial carnitine transferases and carries all of the intermediates of fatty acid β-oxidation in peroxisomes and mitochondria. CoA acyl-thioesters are also the substrates for the acyltransferases and desaturases involved in membrane phospholipid formation, triglyceride synthesis, and protein acylation. Thus, CoA participates in the major anabolic and catabolic pathways critical to cell growth and function.

Pan is phosphorylated by pantothenate kinase (PanK) to yield 4′-phosphopantothenate (P-Pan) in the first enzymatic reaction leading to CoA. PanK activity controls the cellular level of CoA in bacteria (6) and mammals (7, 8), and there are multiple *Pank* genes that are differentially expressed and regulated in mammalian tissues (4, 9–11). The first mammalian gene identified was the mouse *Pank1* gene, which encodes two proteins that differ at the N terminus due to alternative splicing of distinct initiating exons (9). PanK1α enzyme activity is feedback inhibited by both unacylated CoA and acetyl-CoA (9), whereas the PanK1β isoform is less sensitive to feedback regulation by acetyl-CoA and is stimulated by unacylated CoA (8). The human *PANK2* gene also encodes two protein isoforms,

Manuscript received 24 June 2003 and in revised form 3 September 2003.

Published, JLR Papers in Press, October 1, 2003.
DOI 10.1194/jlr.M300279-JLR200

Abbreviations: BF, bezafibrate; HSS, Hallervorden-Spatz syndrome; P-Pan, 4′-phosphopantothenate; P-PanSH, 4′-phosphopantetheine; Pan, pantothenate; PanK, pantothenate kinase; PKAN, pantothenate kinase-associated neurodegeneration; PPARα, peroxisome proliferator activator receptor-α; RACE, rapid amplification of cDNA ends.

[1] The nucleotide sequences reported in this paper have been submitted to the GenBank™/EBI Data Bank with accession numbers AY027661, AY027662, and AY027663.

[2] Present address of M. A. Karim: Division of Endocrinology, Department of Medicine, Central Arkansas Veterans Healthcare System and University of Arkansas for Medical Sciences, Little Rock, AR 72205.

[3] To whom correspondence should be addressed.
e-mail: suzanne.jackowski@stjude.org.

one of which preferentially localizes to mitochondria (11). Mutations in the human *PANK2* coding sequence create a metabolic imbalance leading to either HARP (hypoprebetalipoproteinemia, acanthocytosis, retinitis pigmentosa, pallidal degeneration) syndrome (12) or a progressive childhood neuropathy called PanK-associated neurodegeneration (PKAN) (10) characterized by iron accumulation in the basal ganglia. The human genetic data suggest that dysfunctional CoA biosynthesis due either to defective expression or to sequence alteration of a single PanK isoform can selectively impact the function of specific tissues.

PanK1 is expressed at the highest levels in mouse liver, kidney, and heart tissues (8, 10). Before the discovery of multiple PanK isoforms, it was noted that the levels of liver PanK activity (13, 14) decreased in conjunction with CoA levels following starvation and increased following feeding (15–19), increased in diabetes (20, 21), and increased after treatment with hypolipidemic agents (17, 22, 23), suggesting that changes in PanK expression may be involved in altering the physiological status of the tissues. The peroxisome proliferator activator receptor-α (PPARα) is a transcription factor that is highly expressed in liver, regulates the expression of fatty acid oxidation genes (24), and is activated by hypolipidemic agents such as the fibrates and WY146,43 (25). Activated PPARα binds to the retinoic acid receptor RXR, and this complex binds to specific DNA sequences called peroxisome proliferator response elements (PPREs) located in the promoter regions of target genes to upregulate their expression (26–29).

This work investigates the role of PanK gene expression in regulating CoA biosynthesis in human hepatoblastoma (HepG2) cultured cells. The full-length human *PANK1α* transcript was identified and the human *PANK1* gene structure determined. The human PanK1β isoform (30, 31) is homologous with the mouse PanK1β (8). Like the murine PanK1α isoform, the human PanK1α protein is significantly longer than the human PanK1β at the N terminus. The expressed human PanK1α protein is biochemically active, its expression is stimulated by the PPARα agonist, bezafibrate (BF), and increased PanK1α activity resulted in elevated CoA levels. These data describe a mechanism for stimulation of CoA biosynthesis via increased PanK activity in human liver cells and point to regulation of PanK1α isoform expression as a component of the physiological response to hypolipidemic agents.

EXPERIMENTAL PROCEDURES

Materials

Sources of supplies were as follows: American Radiolabel Co., Inc., D-[1-^{14}C]pantothenic acid (55 mCi/mmol) and D-[2,3-^{3}H]pantothenic acid (25 Ci/mmol); American Type Culture Collection, human HepG2 cells and African Green Monkey kidney (COS7) cells; Amersham Pharmacia Biotech, deoxycytidine 5′-[α-^{32}P]triphosphate (3,000 Ci/mmol), ECL Western blotting detection kit, Rediprime II labeling kit; Analtech, Silica gel H TLC plates; Analytical Luminescence Laboratory/BD Pharmingen, Monolight® 2010 Luminometer; Biodesign International, Saco, ME, sheep anti-bovine catalase antibody; BioWhittaker, Dulbecco's modified Eagle's medium (DMEM) and phenol red-free DMEM; Boehringer Mannheim, RNaseA, terminal transferase; Calbiochem, protease inhibitor cocktail set III, sodium pantothenate, CoA, 4′-phosphopantetheine (P-PanSH); Clontech, Expand long template PCR system, ExpressHyb hybridization solution, Marathon-ready™ liver and kidney cDNA libraries, human brain, heart, kidney, liver, skeletal muscle and testis poly(A)$^+$ RNA; Falcon, culture plasticware; Hyclone, fetal bovine serum (FBS) and 0.25% trypsin; Invitrogen (Gibco) Life Technologies, Inc., cDNA cycle kit, TRIzol LS reagent, TA cloning kit, pcDNA3.1(−) vector, glutamine, penicillin/streptomycin, phosphate-buffered saline, lipofectAMINE™ and lipofectAMINE plus™ reagent, Pan-free DMEM; Jackson ImmunoResearch Laboratories, Inc., West Grove, PA, fluorescein (FITC)-conjugated goat anti-rabbit IgG, RNase A, Texas Red-coupled donkey anti-sheep antibody; Kodak, BioMax MR X-ray films; Media Cybergenetics, Silver Spring, MD, ImageProPlus software; Micron Separations Inc., Nitropure nitrocellulose transfer membranes; Misonix Sonicator 3000; Molecular Dynamics, Storm 860 Phosphor Imager, and Typhoon Phosphor Imager; Molecular Probes, mitotracker red, propidium iodide; Nalge Nunc International, Labtek glass chambers; Novatech, PAN-free DMEM; Promega, pGL3 vectors, restriction endonucleases, Taq polymerase, Luciferase Assay kit; Roche, 5′/3′-rapid amplification of cDNA end (RACE) kit; Schleicher and Schuell, TURBOBLOTTER™ Rapid Downward Transfer System; Sigma Aldrich Chemical Co., delipidated fetal calf serum, dimethyl sulfoxide, BF. All other supplies were reagent grade or better.

Identification of the hPanK1α-specific transcript sequence

Human BACmid AQ076749 was identified by performing a BLAST search using the mouse *Pank1* cDNA (AF347700) as the query. The 5′-end of the *hPANK1α* transcript was found with 5′-RACE using the exon 1α-specific reverse primer, 5′-CGCCACCGACGAGTTTCAACAT-3′, and human kidney poly(A)$^+$ RNA as template for first-strand cDNA synthesis. The homopolymeric tailing of the purified cDNA was perfomed using terminal transferase and dATP according to the manufacturer's instructions. The dA-tailed, first-strand cDNA was used as the template for first round of PCR using exon 1α-specific 5′-GGGAATCAAGTTCTCTGGGCTTGCA-3′ as reverse primer and an oligo (dT) anchor primer, 5′-GACCACGCGTATCGATGTCGACTTTTTTTTTTTTTTTT-3′, as the forward primer. A second round of PCR was performed using the product from the first-round PCR as the template and using a gene-specific nested reverse primer, 5′-GGGCTTTGTATGGCGATGTGAAAACC-3′, and a PCR anchor primer, 5′-GACCACGCGTATCGATGTCGAC-3′, as the forward primer. The PCR product was subcloned into pCR2.1 and the sequence of the product verified. The 129 bp sequence was found to be identical to a portion of the genomic sequence of human BAC AQ076749. Another round of 5′-RACE was performed using human kidney poly(A)$^+$ RNA as the template and using exon 1α-specific reverse primer 5′-GGGCTTTGTATGGCGATGTGAAAACC-3′ and the oligo(dT) anchor primer mentioned above. The second round of PCR was performed using the product from the first round as the template and using a gene-specific nested reverse primer, 5′-GAACCGTTTCAGGAGGAATACGG-3′, and PCR anchor primer as the forward primer. The 184 bp product was subcloned into pCR2.1, and the sequence of the plasmid was determined. This sequence marked the end of the hPanK1α transcript.

Tissue distribution of *hPANK* isoforms

Expression of the *hPANK* genes was evaluated by RT-PCR using the cDNA cycle kit according to the manufacturer's instruc-

tions. First-strand cDNA synthesis mediated by reverse transcriptase was done using a common primer, 5′-ACTTCCGGATGCTCTTCAGG-3′, and poly(A)$^+$ RNAs (1 μg) from human brain, heart, kidney, liver, skeletal muscle, and testis (Clonetech) were used as templates. An aliquot (3 μl) of the RT reaction was used as the template for PCR. PCR detected both hPanK1α and hPanK1β isoforms in a multiplex reaction using the above-mentioned common primer as the reverse primer together with 5′-CTGCGGAGGAGGATGGAC-3′ and 5′-GCCGAAGTGCATTATTTCACA-3′ as hPanK1α- and hPanK1β-specific forward primers, respectively. The thermal cycling program was denaturation at 94°C for 30 s, annealing at 57°C for 30 s, and extension at 72° for 45 s. The total number of thermal cycles was 50. The PCR products were separated on a 1.5% agarose gel. The expected sizes of the hPanK1α and hPanK1β PCR products were 163 bp and 318 bp, respectively.

Isolation of total RNA

HepG2 cells were cultured in 150 mm dishes that were placed on ice, and the cells were scraped into 20 ml cell culture medium. The cell suspension was harvested by centrifugation at 106 *g* for 6 min at 4°C. The media was aspirated, and the pellet was resuspended in 6 ml of RNA lysis buffer [4 M guanidinium thiocyanate, 10 mM Tris-HCl (pH 7.4), 2% β-mercaptoethanol, 2% Sarkosyl, and 10 mM EDTA]. RNA was extracted using the guanidine method (32). Alternatively, RNA was extracted using TRIzol LS reagent according to the manufacturer's instructions.

Detection and quantitation of hPanK isoforms

A primer common to both the hPanK1α and hPanK1β isoforms, 5′-GTCAAATACTTCCGGATGCTC-3′, present in exon 2, was used for first-strand cDNA synthesis by reverse transcription. For hPanK2 and hPanK3, the primers used for cDNA synthesis were 5′-AGCCAATGTTCACCAGAAGC-3′ and 5′-TGACTCCTGAGCCAATGTTC-3′, respectively. The liver fatty acid binding protein (L-FABP) and GAPDH cDNAs were synthesized using 5′-CATGGTATTGGTGATTATGTCGC-3′ and 5′-GACCACCTGGTGCTCAGTGTAG-3′, respectively. RT was done using 2 μg of total RNA as template and the cDNA Cycle Kit according to the manufacturer's instructions. An aliquot of the RT reaction (3 μl) was used as template to amplify the corresponding genes by PCR. An hPanK1 nested reverse primer, 5′-ACTTCCGGATGCTCTTCAGG-3′, was used to amplify both hPanK1α and hPanK1β isoforms by PCR. This primer was present in exon 2 of the *hPANK1* gene. Primers 5′-CTGCTCCCTCAGCATGACTC-3′ and 5′-GACTGAAGCTCATTCAACTGG-3′ were used, respectively, as hPanK1α- or hPanK1β-specific forward primers for PCR. For hPanK2, the forward and reverse PCR primers used were 5′-AGCTGAAGGACCTGACTCTG-3′ and 5′-AGCCAATGTTCACCAGAAGC-3′; for hPanK3, the forward primer was 5′-TATCACAGCAGAGGAAGAGC-3′ and the reverse primer was 5′-TGACTCCTGAGCCAATGTTC-3′; for L-FABP, the forward primer was 5′-GCAGGTCAGTCGTGAAGAGG-3′ and the reverse primer was 5′-CATGGTATTGGTGATTATGTCGC-3′; and for GAPDH, the forward and reverse primers were 5′-CAACAGCCTCAAGATCATCAGC-3′ and 5′-GACCACCTGGTGCTCAGTGTAG-3′, respectively. The thermal cycling program was denaturation at 94°C for 1 min, annealing at 57°C for 30 s, and extension at 72°C for 45 s. Hot start at 94°C for 5 min was done prior to addition of Taq DNA polymerase. Thirty cycles amplified the hPanK isoforms, and 22 cycles amplified for L-FABP and GAPDH, as predetermined to be in the linear range of accumulation of the individual PCR products as a function of cycle time. The sizes of the RT-PCR products were: hPanK1α, 202 bp; hPanK1β, 190 bp; hPanK2, 368 bp; hPanK3, 488 bp; L-FABP, 371 bp; and GAPDH, 424 bp. An aliquot of each PCR reaction (15 μl) was fractionated by electrophoresis on a 1% agarose gel and transferred to Hybond-N$^+$ nylon membrane using the TURBOBLOTTER™ Rapid Downward Transfer System according to the manufacturer's instructions.

The RT-PCR products were detected by Southern hybridization. The PCR products corresponding to the genes were used as template for synthesis of radioactive probes. The probes were labeled with Redivue deoxycytidine 5′-[α-^{32}P]triphosphate using the Rediprime II labeling kit according to the manufacturer's instructions. The blots were hybridized using 2×10^6 cpm/ml of radiolabeled probe in ExpressHyb hybridization solution according to the manufacturer's instructions. Following overnight hybridization, the blots were washed and exposed to phosphor screens for 2 h, and the bands were quantitated using a Storm 860 Phosphor Imager and the ImageQuant software. Alternatively, the PCR products were run on a 1% agarose gel containing 50 μg/ml of ethidium bromide. The ethidium bromide fluorescence was quantitated using the Typhoon Phosphor Imager.

Construction of reporter gene plasmids

*Nhe*I and *Xho*I restriction sites were introduced at the 5′ and 3′ ends, respectively, of the 2,436 bp hypothetical *hPANK1α* promoter region by PCR using 5′-GCTAGCTAATTACCAAGTGCCTCC-3′ and 5′-CTCGAGGCTTGCAGAGAGGAGATG-3′ as forward and reverse primers and using the Expand long template PCR system. The PCR product contained the promoter region plus the transcriptional start site and the untranslated 5′ sequence of exon 1α up to the translational start site. DMSO (5%) was included in the PCR reaction, and human Bacmid AQ076749 was used as the template. The thermal cycling conditions were denaturation at 94°C for 30 s, annealing at 58°C for 30 s, and extension at 72°C for 4.5 min for 40 cycles. The PCR product was cloned into pCR2.1 vector and transformed into *Escherichia coli* strain INVF′α; plasmids from multiple transformants were sequenced at the Hartwell center for Biotechnology at St. Jude Children's Research Hospital. The plasmid with the correct DNA sequence was digested with *Xho*I and subcloned into the pGL3 vector upstream of the luciferase reporter sequence. Plasmid with the promoter in the sense orientation (5′ to 3′) was called P1α, and plasmid with the promoter in the reverse orientation (3′ to 5′) was called P1α-reverse.

Luciferase assays

HepG2 cells were grown to 80% confluence in 6-well plates in phenol red-free DMEM, 10% FBS, and 2 mM glutamine. Cells were transfected with 2 μg of plasmid P1α, P1α-reverse, or pGL3 basic vector; or 0.5 μg of simian virus 40 (SV40)-driven pGL3 promoter vector using lipofectAMINE plus™ reagents according to the manufacturer's instructions. The duration of transfection was 5 h, following which phenol red-free DMEM, 20% delipidated fetal calf serum, and 2 mM glutamine were added. Twenty-four hours post-transfection, the medium was replaced with complete medium containing phenol red-free DMEM, 10% delipidated fetal calf serum, and 2 mM glutamine. The cells were maintained in complete medium for 24 h, following which fresh complete medium was added to the cells. DMSO or BF (0.5 mM) was added to cells. After incubation for 72 h, the cells were analyzed for luciferase activity using the Luciferase Assay kit according to the manufacturer's instructions. Luciferase activity was measured in the Monolight® 2010 Luminometer. Data were normalized to protein content in the lysate as determined by the Bradford method (33).

Cloning and assembly of hPanK1α cDNA

Based on the sequence information, 5′-GCTAGCTTCACATCGCCATACAAAGCC-3′ and 5′-CCATGGGAATGGCGGCCT-

GTTCTTTCTCCC-3′ were used as *hPANK1α*-specific primers to introduce *Nhe*I and *Nco*I restriction endonuclease sites at the 5′- and 3′- ends of exon 1α. PCR-mediated cDNA synthesis was performed using human Bacmid AQ076749 as the template, and the product was called Fragment 1 and was cloned into pCR2.1. Human liver Marathon-Ready™ cDNA was used as template to perform 5′-RACE using the human *PANK1* gene-specific reverse primer 5′-CTCGCTGCCCATCTGAATGAACC-3′ and an adaptor primer, 1, 5′-CCATCCTAATACGACTCACTATAGGGC-3′, as the forward primer for the first round of cDNA synthesis. The cDNA product from the first round was used as a template for the second round of PCR-mediated cDNA synthesis using a nested *hPANK1* gene-specific forward primer, 5′-GGACGTCTCGGATCCCAG-3′, and a nested adaptor primer, 2, 5′-ACTCACTATAGGGCTCGAGCGGC-3′. This fragment contained exon 1β and a portion of exon 2 of the *hPANK1* gene and was called Fragment 2 and was cloned into pCR2.1. PCR-mediated cDNA synthesis was performed using human kidney Marathon-Ready™ cDNA as template and *hPANK1*-specific forward and reverse primers 5′-CGTCCACCTGGAACTGAAAAACCTG-3′ and 5′-CCGAGCAATGGAGCCAATG-3′, respectively. A 724 bp cDNA fragment corresponding to exon 2 was obtained. *Aat*II and *Bst*UI restriction enzyme sites were introduced at the 5′- and 3′- ends, respectively, of this 724 bp product by PCR using 5′-GACGTCCACCTGGAACTGAA-3′ and 5′-CGCGCACATCCGAGCAATGG-3′ as forward and reverse primers. This fragment was called Fragment 3 and was cloned into pCR2.1. Poly(A)$^+$ RNA from human kidney was used as a template to perform 3′-RACE using an oligo(dT)-containing adaptor primer 5′-GGCCACGCGTCGACTAGTACTTTTTTTTTTTTTTTT-3′ for reverse transcription, and the resulting cDNA was used as template for PCR-mediated cDNA synthesis using the *hPANK1* gene-specific forward primer 5′-CATTGGCTCCATTGCTCGG-3′ and the abridged universal amplification primer 5′-GGCCACGCGTCGACTAGTAC-3′ as the reverse primer. A 1,676 bp RT-PCR product was obtained and contained exon 6 and the coding region of exon 7. A *Bst*EII site was introduced at the 5′-end of this cDNA product by PCR-mediated cDNA synthesis using 5′-TGGTCACCATCACCAACAACATTGGCTCCATTGCTCGG-3′ as the forward primer and 5′-GCGGCCCCGACTTTCACCTTCTCCAGCAG-3′ as the reverse primer. This 313 bp PCR product was called Fragment 4 and was cloned into pCR2.1. Multiple independent transformants were isolated from each PCR cloning, and the DNA sequences of the plasmids were determined using M13 forward and reverse primers at the Hartwell Center for Biotechnology at St. Jude Children's Hospital.

Fragments 1, 2, 3, and 4 were assembled and cloned into pcDNA3.1(−), a mammalian expression vector. First, Fragment 2 was subcloned into pBluescriptKS(+/−) using unique *Spe*I and *Xho*I restriction sites. Next, Fragment 1 in pCR2.1 and Fragment 2 in pBluescriptKS(+/−) were digested with *Kpn*I and *Nco*I. The 823 bp product obtained from digestion of Fragment 1 contained exon 1α and was ligated to the 3,045 bp fragment obtained from the digestion of Fragment 2 in pBluescriptKS(+/−), which lacked exon 1β. The ligated product, called "1+2", was transformed into *E. coli* strain INVF′α. Fragments 3 and 4, each cloned into pCR2.1, were digested with *Xba*I and *Bst*EII. The 738 bp product from the Fragment 4 plasmid was ligated into the 4,168 bp product from the Fragment 3 plasmid. The ligated product was called "3+4" and was transformed into INVF′α cells. Fragment 3+4 was then subcloned into pBluescriptKS(+/−) using *Spe*I and *Xho*I restriction sites. The complete *hPANK1α* cDNA was assembled by digesting Fragments 1+2 and 3+4 with *Kpn*I and *Aat*II. The 977 bp product obtained from the Fragment 1+2 digestion was ligated into the 3,937 bp product obtained from the digestion of Fragment 3+4. The ligated product was transformed into INVF′α cells. Finally, the assembled *hPANK1α* cDNA in pBluescriptKS(+/−) was digested with *Nhe*I and *Xba*I. The 1,984 bp *hPANK1α* cDNA insert was ligated into the 5,304 bp pcDNA3.1(−) vector, which had been digested with *Nhe*I and *Xba*I. The ligated product was transformed into *E. coli* strain INVF′α.

Cell transfection and PanK assays

COS7 cells were cultured in DMEM plus 10% FBS and grown to 80% confluence in 100 mm culture dishes. COS7 cells were transfected with 10 μg of plasmid DNA using lipofectAMINE™ reagent according to the manufacturer's instructions. Cells were harvested 48 h after transfection and were resuspended in hypotonic lysis buffer [10 mM Tris (pH 7.5), 1 mM EDTA, 1× protease inhibitor cocktail set III], incubated on ice for 30 min, and lysed by sonication at maximum power for 3 min in 30 s pulses at 4°C. The cell lysate was centrifuged at 5,500 *g* for 10 min at 4°C, and the supernatant was used for PanK assays. The assay mixture contained 100 mM Tris (pH 7.5), 20 mM $MgCl_2$, and freshly made 1 mM ATP and D-[1-[^{14}C]pantothenic acid (50.5 μM; specific activity, 55 mCi/mmol) plus the indicated amount of lysate protein and was incubated at 37°C for 15 min. The assay was stopped, and the P-Pan product was quantitated as described previously (8).

PanK activity in HepG2 cells was determined as follows: cells were scraped from culture dishes and washed with PBS, and the cell pellets were resuspended in an equal volume of ice-cold hypotonic lysis buffer and incubated in a rotator at 4°C for 1 h. The cells were then lysed by sonication at maximum power for 6 min in 30 s pulses at 4°C. The cell lysate was centrifuged at 5,500 *g* for 10 min at 4°C. The supernatant protein was quantitated by the Bradford method (33) and was used for PanK assays. The PanK assay was performed as described above.

Immunological detection of hPanK1α protein

A peptide ECYYGENPTNPELCQ was synthesized and coupled to keyhole limpet hemocyanin by the Hartwell Center for Biotechnology, St. Jude Children's Research Hospital, and was sent to Rockland Inc., Gilbertsville, PA for raising rabbit polyclonal antiserum against PanK1. Affinity purification of the polyclonal antisera was performed as described previously (9). COS7 cells were transfected and lysed using hypotonic lysis buffer as described above. Aliquots of the crude cell lysate from transfected and untransfected cells were fractionated by SDS-PAGE on 10% gels. The separated proteins were electroblotted onto nitrocellulose membrane, and the hPanK1α protein was detected by immunoblotting using the ECL detection kit according to the manufacturer's instructions. PanK1-specific antibody was used at a dilution of 1:500 (stock 0.4 mg/ml) as the primary antibody, which was incubated with the membrane for 1 h at room temperature. Horseradish peroxidase-labeled anti-rabbit IgG was used as the secondary antibody and was diluted to 1:5,000 prior to incubation with the membrane for 1 h at room temperature. The blots were washed five times with 100 ml of TBS-T and developed using the ECL detection reagents according to the manufacturer's instructions. The chemiluminescent signal was detected using X-ray films.

Immunostaining, confocal microscopy, and quantitation of hPanK1 protein expression

HepG2 cells were seeded at a density of 5×10^4 in DMEM plus 10% FBS in 2-well Labtek glass chambers with DMSO alone or DMSO with 0.5 mM BF (0.25 M stock solution made in DMSO) for indicated times of incubation at 37°C in 5% CO_2, 95% air. The cells were washed with PBS (pH 7.4) three times for 2 min each and permeabilized in 0.5% Triton X-100 in PBS for 5 min at room temperature. The cells were fixed with 4% formaldehyde

in PBS for 30 min at room temperature and incubated with 1% BSA in PBS for 1 h to block nonspecific cellular binding sites. The cells were incubated with the affinity-purified rabbit polyclonal anti-PanK1 primary antibody at the indicated dilutions in PBS for 45 min at 37°C. The anti-PanK1 antibody was removed, and cells were washed five times with PBS. FITC-conjugated goat anti-rabbit IgG (Jackson ImmunoResearch Laboratories, Inc.) diluted 1:50 in PBS was added to the cells, followed by incubation at 37°C for 45 min. The cells were again washed five times with PBS. For nuclear staining, cells were first treated with 1:100 dilution of RNase A [10 mg/ml stock in 10 mM Tris (pH 7.5), Jackson ImmunoResearch Laboratories, Inc.] for 20 min at 37°C to digest RNA, followed by incubation with 5 μg/ml propidium iodide for 5 min at 37°C. The RNase digestion was performed to eliminate nonspecific staining of RNA by propidium iodide. At this point, the plastic chambers on slides were removed, the slides were washed with PBS, and a drop of p-phenylenediamine medium (34) was added to the slides to prevent bleaching of the fluorochrome. The slides were then covered with glass coverslips and sealed with nail polish. In double-staining experiments to localize hPanK protein in mitochondria or peroxisomes, the cells were first stained for the protein, followed by incubation with mitotracker red (Molecular Probes, Eugene, OR) or anti-catalase (sheep anti-bovine catalase antibody; Biodesign International) and Texas Red-coupled donkey anti-sheep antibody (Jackson ImmunoResearch Laboratories, Inc.).

The images were obtained using a Leica TCS NT SP confocal microscope. The microscope is equipped with an argon laser to detect green (FITC) fluorescence (absorption/emission = 494 nm/518 nm) and a Krypton laser to detect red (propidium iodide or Texas Red) fluorescence (absorption/emission = 568 nm/615–617 nm). Single optical sections (0.5 μm thick) were obtained from cells, and the images were sequentially scanned to minimize cross-talk between the green and red channels. Individual sections or three-dimensional images constructed from multiple optical sections were used to display the data in both green and red channels using the Leica imaging software. Overlay images from green and red channels were used to show the colocalization of the two fluorochromes. To maintain consistency and accuracy, samples were examined at the same laser power and at the same photo multiplier tube gain settings in both channels.

The quantitation of hPanK1 protein expression was done using a previously described procedure (35) and ImageProPlus software (Media Cybergenetics). Mean fluorescence intensity (FITC-green) of the hPanK1 protein signal in the cytoplasm was measured in control cells and in those treated with BF. Single-section digital images containing 20 cells were used in the analysis to determine the fluorescence intensity of the cytoplasm (single pixel intensity × number of pixels per cell); the nuclei, defined by the red fluorescence of the propidium iodide, were excluded from the analysis.

Metabolic labeling

HepG2 cells were grown to 35% confluence in 100 mm culture dishes in regular complete DMEM plus 10% serum. Cells were washed twice with PBS and radiolabeled with D-[2,3-^{3}H]pantothenic acid (33.3 nM, specific activity 25 Ci/mmol) in PAN-free DMEM. At the times indicated, cells were washed with PBS and harvested by trypsinization using 0.25% trypsin. Following inactivation of the trypsin, the cells were separated from the medium and cell pellets were stored at −80°C. The pellets were resuspended in 50 μl of hypotonic lysis buffer and lysed by sonication as described above. The cell lysate was centrifuged at 10,620 *g* for 10 min at 4°C. Aliquots (10 μl) of the lysates were treated with DTT for 3 min and spotted onto silica gel H TLC plates to separate the radiolabeled metabolites. The plates were developed with butanol-acetic acid-water (5:2:4; v/v/v) as the solvent system. Plates were scraped (0.5 cm zones) into scintillation vials, and radioactivity was counted following deactivation of the silica gel and addition of scintillation fluid. The metabolites were identified and quantified by comigration with authentic standards for Pan, CoA, and P-PanSH (6).

RESULTS

Structure of the human *PANK1* gene

A BLAST search of the National Center for Biotechnology Information human genomic database identified a high throughput genomic contig, AL157400, that resembled the mouse *Pank1* cDNA and gene structure (9). A comparison of the mouse and human PanK1α DNA sequences suggested, however, that the human PanK1α open reading frame was longer than the mouse protein due to the absence of a translational initiating methionine preceded by upstream stop codons. Thus, the complete cDNA sequence of hPanK1α was determined using 5′-RACE, RT-PCR, and 3′-RACE techniques as described under Experimental Procedures. Compared with mPanK1α, the hPanK1α transcript encoded an additional 38 amino acids at the N terminus of the protein, and in-frame stop codons were located upstream of the initiating methionine. The structure of the human *PANK1* gene was determined by comparing the human *PANK1α* and *β* cDNA sequences with the genomic sequence of AL157400 (**Fig. 1**; **Table 1**). The *hPANK1α* transcript initiates at exon-1α, which consists of 989 bp: 705 bp constitute the coding region, and the remaining 284 bp constitute the 5′-untranslated region. *hPANK1β* initiates at exon-1β, which consists of 195 bp: 30 bp of coding sequence, with the remaining 165 bp constituting the 5′-untranslated region. Either of these exons are spliced into exons 2 through 7, which are common to both the transcripts. The common exon 7 consists of 1,478 bp, which includes 1,421 bp of 3′-untranslated region as determined by 3′-RACE. The *hPANK1α* transcript is 3.5 kb, and the *hPANK1β* transcript is 2.7 kb. The *PANK1* gene was mapped to human chromosome 10q23.3-23.31 based on the human genome project, and this location was confirmed by fluorescence in situ hybridization using human BACmid AQ076749 as the probe (data not shown). In summary, the human *PANK1* gene encodes two protein isoforms, PanK1α and PanK1β. The *hPANK1α* open reading frame encodes a protein of 598 amino acids, whereas the *hPANK1β* encodes a 373 amino acid protein (**Fig. 2**). These proteins differ in their amino termini but share a common carboxy terminal domain consisting of 363 amino acids.

Tissue distribution of the human *PANK1* isoforms

Poly(A)$^+$ RNA isolated from various human tissues was used as template in a multiplex RT-PCR experiment to determine the relative expression levels of *hPANK1α* and *hPANK1β* mRNAs (**Fig. 3**). *hPANK1α* mRNA was expressed in brain, heart, kidney, liver, skeletal muscle, and testis, whereas *hPANK1β* was expressed in much lower lev-

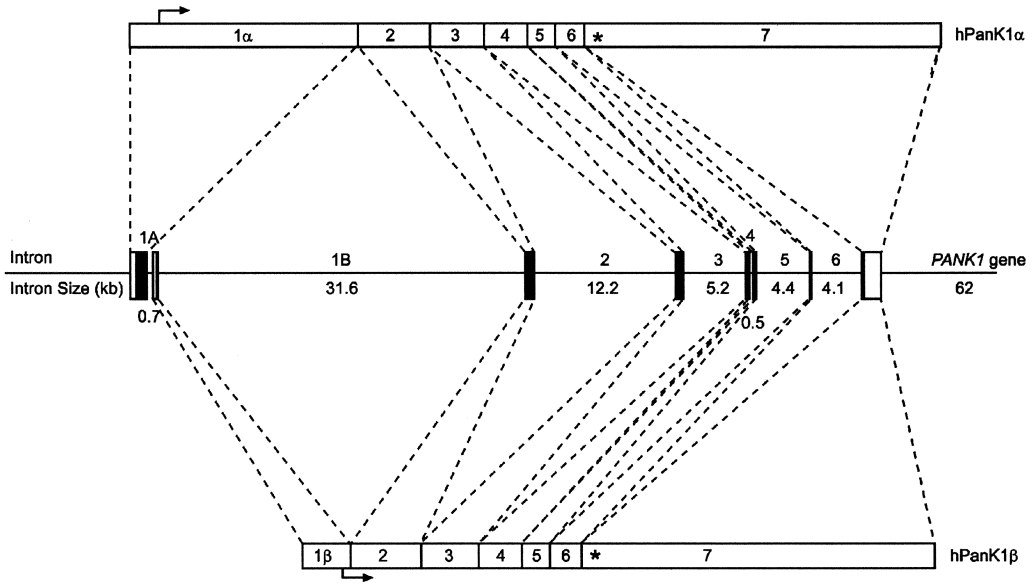

Fig. 1. Diagram of the human *PANK1* gene structure. The exon/intron arrangement of the 62 kb human *PANK1* gene is diagrammatically illustrated along with the *hPANK1α* and *hPANK1β* transcripts that encode distinct PanK1 proteins. The two hPANK1 isoforms differ at exon 1 and utilize common exons 2–7. The darkened boxes depict the coding regions within the exons, and the lighter boxes indicate the untranslated sequences. The diagram is not to scale, and the approximate intron sizes are indicated. The exact sizes of the introns and exons are listed in Table 1. The arrows indicate the translational start sites. The translational stop sites are depicted by the asterisks.

els in kidney, liver, brain, and testis, and was not detected in heart and skeletal muscle. The control lane illustrates the expected PCR products using *hPANK1α* and *hPANK1β* cDNA expression plasmids as templates.

hPANK expression in HepG2 cells

Cultured HepG2 cells were chosen for investigation because the *PANK1α* and *PANK1β* isoforms are expressed (see below) in this commonly used cell line, in which fatty acid metabolic gene expression is responsive to PPARα-activating ligands (36). Cells were incubated with BF, a PPARα agonist, at concentrations up to 0.7 mM in complete medium containing 10% serum for 24 h. BF binds to serum components (37), and the BF concentrations used in our work matched those required for a genetic response in this system (38). Incubation with BF at the concentrations indicated did not change the doubling time or confluent cell density of the HepG2 cells (data not shown). Relative expression levels of the *hPANK* isoforms and the *L-FABP*- and *GAPDH*-positive and negative control genes, respectively, were determined by semiquantitative RT-PCR. The basal *PANK1α* was expressed at a 2-fold higher level compared with *PANK1β* using this assay. The *hPANK1α* mRNA increased significantly in response to 0.5 mM BF (**Fig. 4A**, **B**) and increased up to 5-fold following treatment with 0.7 mM of the drug. In contrast, the levels of *hPANK2* and *hPANK3* did not change, and *hPANK1β* decreased slightly following incubation with the drug. *L-FABP* mRNA expression was significantly enhanced in response to increasing concentrations of the agonist (Fig. 4A, C), as reported previously for this PPARα-responsive gene (9), whereas *GAPDH* remained unchanged (Fig. 4A). These data show that BF increased the expression of PPARα target genes in the HepG2 cell system and that *hPANK1α* was the only *PANK* isoform that responded to BF in a dose-dependent manner.

hPANK1α mRNA exhibited a detectable increase at 12 h following 0.5 mM BF treatment, and reached a maximum at 24 h that was maintained at 48 h (**Fig. 5A**, **B**). However, the levels of *hPANK2* and *hPANK3* expression did not change in response to the drug, and the *hPANK1β* message decreased slightly (Fig. 5A, B), in agreement with the BF dose response shown in Fig. 4. The relative level of the control *L-FABP* mRNA increased following 6 h of BF treatment and was about 6-fold higher after 24 h (Fig. 5A, C).

TABLE 1. The human *PANK1* gene: splice junctions, exons, and introns

Exon	Length	Splice Donor Site[a]	Splice Acceptor Site	Intron	Length
	bp				*Kb*
1α	989	GGCCGCgtaagt	ctttagCATTCC	1A	0.7
1β	195	AGCAAAgtaagt	ctttagCATTCC	1B	31.6
2	353	AGAATGgtaggt	ttttagATTGCT	2	12.2
3	254	GACCAGgtaaac	cttcagTCTTGG	3	5.2
4	177	ATCAAGgtagag	acatagCTTTGG	4	0.5
5	124	AATGAGgtaagg	ttccagAACATA	5	4.4
6	126	CATGAGgtaggt	tcgtagGGTTAT	6	4.1
7	1478	CTGTTGTG(Poly A)			

[a] Exon sequences are represented in upper-case and introns in lower-case letters. Splice donor and acceptor sites of all the introns conformed to the consensus GT-AG rule.

```
hPanK1α      MLKLVGGGGGQDWACSVAGTSLGGEEAAFEVARPGDQGKAGGGSPGWGCAGI
hPanK1β

hPanK1α      PDSAPGAGVLQAGAVGPARGGQGAEEVGESAGGGEERRVRHPQAPALRLLNRK
hPanK1β

hPanK1α      PQGGSGEIKTPENDLQRGRLSRGPRTAPPAPGMGDRSGQQERSVPHSPGAPVG
hPanK1β

hPanK1α      SAAVNGLLHNGFHPPPVQPPHVCSRGPVGGSDAAPQRLPLLPELQPQPLLPQH
hPanK1β

hPanK1α      DSPAKKCRLRRRMDSGRKNRPPFPWFGMDIGGTLVKLVYFEPKDITAEEEQEEV
hPanK1β                   MKLINGKKQTFPWFGMDIGGTLVKLVYFEPKDITAEEEQEEV

hPanK1α      ENLKSIRKYLTSNTAYGKTGIRDVHLELKNLTMCGRKGNLHFIRFPSCAMHRFI
hPanK1β      ENLKSIRKYLTSNTAYGKTGIRDVHLELKNLTMCGRKGNLHFIRFPSCAMHRFI

hPanK1α      QMGSEKNFSSLHTTLCATGGGAFKFEEDFRMIADLQLHKLDELDCLIQGLLYVD
hPanK1β      QMGSEKNFSSLHTTLCATGGGAFKFEEDFRMIADLQLHKLDELDCLIQGLLYVD

hPanK1α      SVGFNGKPECYYFENPTNPELCQKKPYCLDNPYPMLLVNMGSGVSILAVYSKDN
hPanK1β      SVGFNGKPECYYFENPTNPELCQKKPYCLDNPYPMLLVNMGSGVSILAVYSKDN

hPanK1α      YKRVTGTSLGGGTFLGLCCLLTGCETFEEALEMAAKGDSTNVDKLVKDIYGGDY
hPanK1β      YKRVTGTSLGGGTFLGLCCLLTGCETFEEALEMAAKGDSTNVDKLVKDIYGGDY

hPanK1α      ERFGLQGSAVASSFGNMMSKEKRDSISKEDLARATLVTITNNIGSIARMCALNE
hPanK1β      ERFGLQGSAVASSFGNMMSKEKRDSISKEDLARATLVTITNNIGSIARMCALNE

hPanK1α      VSMKLLANIDRVVFVGNFLRINMRATLVTITNNIGSIARMCALNENIDRVVFVG
hPanK1β      VSMKLLANIDRVVFVGNFLRINMRATLVTITNNIGSIARMCALNENIDRVVFVG

hPanK1α      NFLRINMYAMDFWSKGQLKALFLEHEGYFGAVGALLELFKMTDDK
hPanK1β      NFLRINMYAMDFWSKGQLKALFLEHEGYFGAVGALLELFKMTDDK
```

Fig. 2. Comparison of hPanK1α and hPanK1β protein sequences. The primary sequences are aligned and illustrate the 235 residue N terminus of hPanK1α, compared with the 10 amino acid N terminus of hPanK1β. The darkened residues indicate the identical residues encoded by exons 2–7.

These results indicated that the specific expression of *hPANK1α* mRNA was responsive to a PPARα agonist in a time-dependent manner.

hPanK1α mRNA half-life

Increased mRNA stability in response to BF treatment may have accounted for the accumulation of *hPANK1α*. This point was tested by treating HepG2 cells with 0.5 mM BF or DMSO (vehicle control) for 20 h, then adding actinomycin D (5 μg/ml) to inhibit further RNA synthesis. RNA samples were prepared at time intervals up to 1 h following actinomycin D treatment, and the *hPANK1α* mRNA levels were determined by RT-PCR (**Fig. 6**). GAPDH mRNA expression was chosen both as an RNA loading control and as a negative control for actinomycin D treatment, because the half-life of GAPDH message is greater than 20 h in HepG2 cells (39, 40). The level of *hPANK1α* message decreased with actinomycin D at the same rate in both control and BF-treated cultures (Fig. 6A, B) to about 23% of the initial amount after 1 h of treatment. The mRNA half-lives were determined from the slopes of the lines obtained by linear regression analysis, and there was no significant difference between the *hPANK1α* message stability in control (40 min) or BF-treated cells (35 min). These data ruled out decreased mRNA degradation as a mechanism for heightened *hPANK1α* mRNA levels following BF treatment.

Response of the *hPANK1α* promoter to a PPARα agonist

We next investigated the role of the *hPANK1α* promoter in the increased expression of hPANK1α mRNA in response to BF. Genomic DNA sequence (2.4 kb) 5′ to the transcript start site, called the "*PANK1α* promoter" region, was evaluated for common promoter sequences and PPRE(s). Four putative PPREs were identified in the *PANK1α* promoter region (**Fig. 7A**), with midpoints at

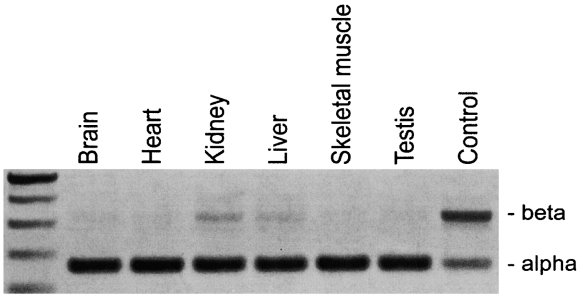

Fig. 3. Tissue distribution of *hPANK1α* and *hPANK1β* transcripts. Poly(A)$^+$ RNAs from various human tissues were screened using RT-PCR to detect the two PANK1 mRNAs as described under Experimental Procedures. The two transcripts were detected using a common reverse primer and an isoform-specific forward primer. The expected sizes of the *hPANK1α* and *hPANK1β* PCR products were 163 bp and 318 bp, respectively. Plasmids containing the *hPANK1α* and *hPANK1β* cDNAs were used as positive controls.

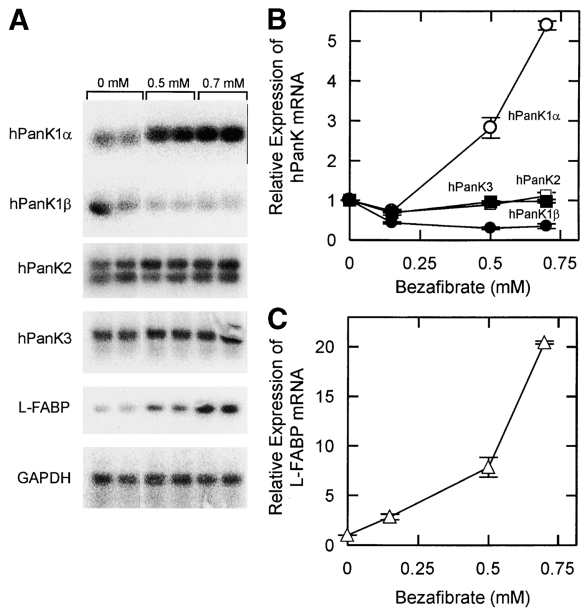

Fig. 4. Bezafibrate (BF) stimulates *hPANK1α* mRNA expression. Hepatoblastoma (HepG2) cells were treated with 0 mM, 0.15 mM, 0.5 mM, and 0.7 mM BF for 24 h. Total RNA was extracted and used for RT-PCR, Southern blot detection, and quantitation as described under Experimental Procedures. The expression of *hPANK* and *L-FABP* transcripts at each concentration of BF was normalized to that of GAPDH mRNA. A: Detection of RT-PCR products by Southern hybridization. The experiments were performed at least twice in duplicate, and a representative Southern blot is shown in A. B: Quantitation of the expression of *hPANK1α* (open circle), *hPANK1β* (closed circle), *hPANK2* (open square), and *hPANK3* (closed square) transcripts relative to GAPDH as a function of BF concentration. C: Expression of the control peroxisome proliferator activator receptor-α-responsive *L-FABP* mRNA (triangle) relative to GAPDH. The untreated mRNA-GAPDH ratio was set at 1.0. The error bars in B and C represent duplicate data points.

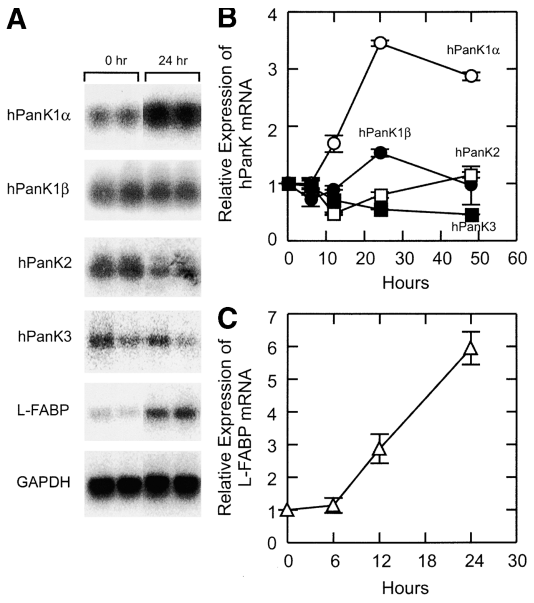

Fig. 5. Time-dependent BF stimulation of *hPANK1α* expression. HepG2 cells were treated with 0.5 mM BF for 0 h, 6 h, 12 h, 24 h, and 48 h. Total RNA was extracted and used for RT-PCR and Southern blot detection and quantitation as described under Experimental Procedures. hPANK and liver fatty acid binding protein (L-FABP) transcripts were quantified and normalized to GAPDH expression at each time point with the zero time control ratios set at 1.0. A: Detection of RT-PCR products by Southern hybridization. B: Expression of *hPANK1α* (open circle), *hPANK1β* (closed circle), *hPANK2* (open square), and *hPANK3* (closed square) transcripts relative to GAPDH as a function of BF concentration. C: Expression of *L-FABP* mRNA (triangle) relative to GAPDH. The experiments were performed twice in duplicate, and a representative Southern blot is shown in A. The error bars in B and C represent duplicate data points.

−771 bp, −1,210 bp, −1,370 bp, and −2,141 bp relative to the transcription start site, which was defined as 0 bp. The putative PPRE present at −1,370 bp matched 100% with the consensus for the human PPRE (41), and the remaining three PPREs deviated from the consensus by one base pair. Reporter gene constructs containing the 2.4 kb of putative promoter sequence (Fig. 7A) plus the untranslated region of exon 1α were made by subcloning the genomic DNA in the sense (P1α) and the anti-sense (P1α-reverse) orientations relative to the luciferase open reading frame in the pGL3− vector. The activity of the promoter region in both orientations was determined by luciferase assays in HepG2 cell lysates following transfection with the reporter constructs. P1α promoter activity was clearly evident in cells transfected with the sense construct (Fig. 7B), and this activity doubled upon treatment with 0.5 mM BF (Fig. 7B). The P1α promoter cloned in the reverse orientation was inactive. The activities of the pGL3− vector lacking promoter sequences (negative control) and the pGL3+ vector containing the SV40 promoter upstream of the luciferase open reading frame (positive control) did not change in response to the drug. These results indicated that the *hPANK1α* promoter activity increased in cultured HepG2 cells following treatment with BF, consistent with the BF-elevated *hPANK1α* mRNA. These data support the conclusion that PPARα elevates *hPANK1α* expression in response to BF via one or more of the PPREs located in the promoter region.

Analysis of the *PANK1α* promoter using the TRANSFAC database (42) revealed the presence of additional binding sites for transcription factors involved in the regulation of carbohydrate and lipid metabolism. A putative carbohydrate response element was present at −1,110 bp. A carbohydrate response element is present in the promoter of glycolytic genes such as pyruvate kinase and lipogenic genes such as S14 (43–46). A putative sterol-regulatory element binding protein (SREBP) site was present at −1,075 bp. This site is present in the promoter regions of genes involved in coordinating glucose and lipid metabolism (46–48). A putative glucose response element (GlRE) or upstream stimulatory factor binding site (E-box) was found at −337 bp, similar to the GlRE identified in a PPARα promoter (49, 50). This analysis suggests that several other regulatory factors may control hPanK1α expression. In particular, the regulation by glucose through the GlRE element and by lipids via the SREBP1 site appear to be the most important to investigate in the future in light of the cen-

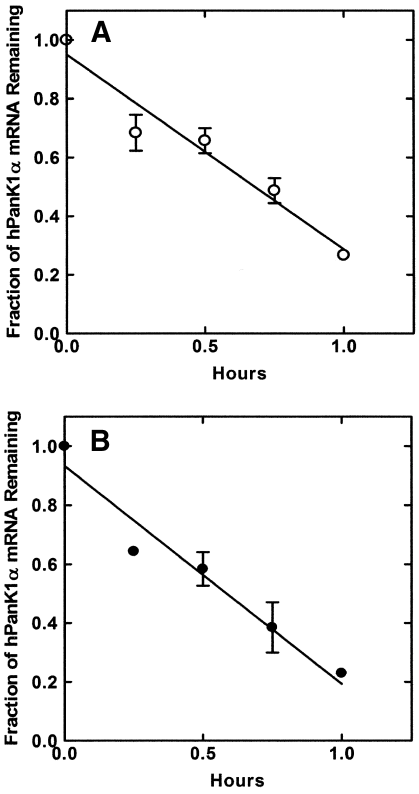

Fig. 6. *hPANK1α* mRNA stability following BF treatment. HepG2 cells were treated with DMSO or with 0.5 mM BF for 20 h followed by treatment with 5 μg/ml actinomycin D for 0 min, 15 min, 30 min, 45 min, and 60 min. Total RNA was isolated, and *hPANK1α* and GAPDH mRNAs were determined by RT-PCR, followed by ethidium-bromide staining and quantification of the fluorescent products using a Typhoon™ Phosphor Imager as described under Experimental Procedures. *hPANK1α* mRNA values were normalized to GAPDH mRNA and the ratio set at 1.0 at 0 h in the absence of actinomycin D. A: DMSO-treated cells, 40 min half-life. B: BF-treated cells, 35 min half-life. The results are plotted from two independent turnover experiments. The error bars represent triplicate data points.

tral importance of CoA to lipid and carbohydrate metabolism.

hPANK1α cDNA encodes a functional PanK

The human *PANK1α* open reading frame is larger than the homologous mouse sequence and encodes an additional 38 amino acids at the N terminus of the protein. To confirm that the larger human PanK1α protein was, in fact, active in the cellular context, the cDNA was assembled and cloned into pcDNA3.1(−), a mammalian expression vector. The hPanK1α protein is made up of 598 amino acids (Fig. 2), with 235 amino acids arising from exon 1α and the remaining 363 amino acids derived from exons 2 through 7 (Fig. 1). The calculated molecular mass of the protein is 65.8 kDa. COS7 cells were transfected with the hPanK1α cDNA, and cell lysates were analyzed for PanK enzyme activity (**Fig. 8A**). The *hPANK1α*-transfected cells exhibited significantly higher PanK-specific activity, compared with control cells transfected with vector plasmid alone. Control COS7 cell lysates had very low activity, detectable only at concentrations >250 μg protein (data not shown). Our affinity-purified rabbit polyclonal PanK1 anti-peptide antibody detected the hPanK1 protein in the crude lysate from *hPANK1α*-transfected cells with an estimated size of 66 kDa (Fig. 8B), consistent with the calculated size from the cDNA sequence. The endogenous protein was not detected using the immunoblotting technique at protein loads up to 88 μg/lane (not shown). This observation is consistent with the low enzyme-specific activity in cell lysates (see below) and indicates that hPanK1 is not an abundant protein in HepG2 cells. This conclusion is consistent with a rate-controlling role for PanK1 in the CoA biosynthetic pathway.

BF elevated hPanK1 protein levels in HepG2 cells

HepG2 cells were treated with DMSO or BF for 72 h and examined for the expression and localization of hPanK1 protein using immunofluorescence and confocal microscopy (**Fig. 9**). The cells exhibited fluorescence in the cytoplasm (green fluorescence, Fig. 9, left); the nuclei were stained red with propidium iodide (Fig. 9, middle), and the overlay of the two probes is shown in Fig. 9, right. The fluorescence pattern is largely diffuse, with some punctate staining, indicating that the majority of protein is cytosolic. The punctate staining suggested that a portion of the protein may be associated with a subcellular organelle. However, we do not think that this is the case, because double staining of the cells with anti-hPanK1 antibody and mitotracker dye (specific for mitochondria) or anti-catalase antibody (specific for peroxisomes) showed that the majority of hPanK1 did not localize with the mitochondrial or peroxisomal markers (data not shown), and the punctate staining remained in the following controls. Two control experiments were performed to determine if components of the hPanK1 staining were nonspecific. First, the PanK1 antibody was preincubated with the peptide epitope prior to staining the cells. These results (Fig. 9G, H, I) show a significant reduction in total fluorescence, confirming that the majority of the signal arose from antibody binding to the hPanK1 epitope. Second, the extent of nonspecific staining by the FITC-coupled secondary antibody was determined by incubation with this secondary antibody alone. These results showed even lower levels of cytoplasmic fluorescence with secondary antibody alone (Fig. 9J, K, L). In both controls, the punctate green fluorescence was present while the diffuse cytoplasmic green fluorescence was not present, leading to the conclusion that hPanK1 protein was cytoplasmic and the punctate staining was nonspecific.

The levels of hPanK1 were quantitated in control and BF-treated cells by measuring the fluorescence intensities in confocal images (**Fig. 10**). Measurements were made in cells treated with either DMSO or BF at intervals between 0 h and 72 h and the relative fluorescent intensities plotted. In cells treated with BF, the expression of hPanK1 protein increased by a factor of 1.7 at 24 h and was maintained at this elevated level up to 72 h (see also Fig. 9D, E, F). The protein levels did not significantly change between 0 h and 72 h in DMSO-treated cells. These data are

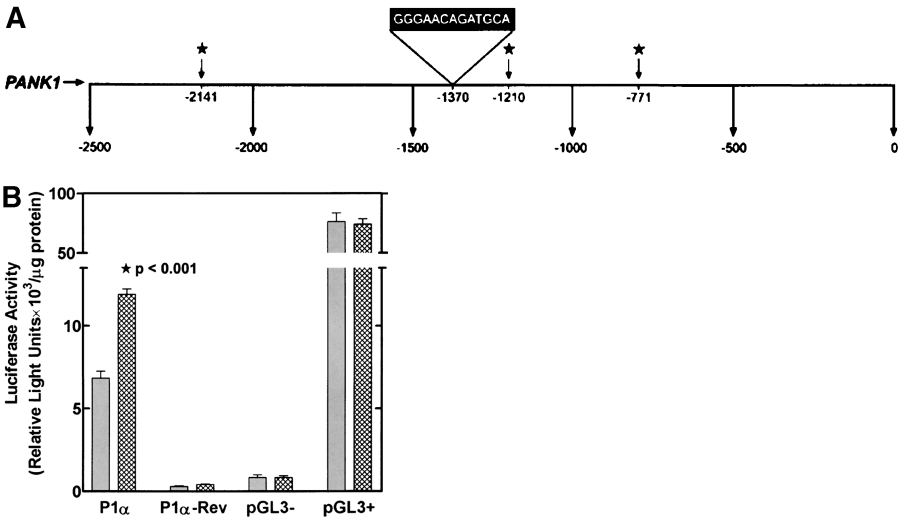

Fig. 7. Analysis of the *hPANK1α* promoter region. A: Putative peroxisome proliferator response elements (PPREs) in a 2.4 kb DNA sequence 5′ to the transcript start site are indicated. The transcriptional start site is numbered as 0 and the positions of the upstream bases are indicated by negative numbers. The midpoints of the sequences of the PPREs are 5′-AGACTCTGACTCC (−771 bp), 5′-GGAGTCATAAACAGA (−1,210 bp), 5′-GGGAACAGATGCA (−1,370 bp), and 5′-AGGGATAGAGTGA (−2,141 bp). The human PPRE consensus sequence is (A/G, G, G/A, N, C/A/T/G, A/C/G, A/C/G/T, A/G/C, G/T/A, G/T, T/G, C/G, A/C). B: HepG2 cells were transfected with *hPANK1α* promoter-luciferase reporter plasmids constructed in the sense (P1α) and antisense (P1α-Rev) orientation and treated with 0.5 mM BF 48 h later. Luciferase activity was measured at 72 h and normalized to cell lysate protein amount in each sample. Gray bars represent the luciferase activity in DMSO-treated cells; cross-hatched bars represent luciferase activity in cells treated with 0.5 mM BF. The simian virus 40 promoter vector (pGL3+) is a positive activity control; the pGL3(−) is a vector control lacking promoter sequence. The error bars represent triplicate data points, and the *P* value ($P < 0.001$) was determined using the Sigmastat program. The results are derived from two independent experiments.

consistent with an increase in cellular PanK1 protein occurring in response to BF treatment.

BF increased cellular PanK-specific enzyme activity

HepG2 cells were treated with DMSO or 0.5 mM BF for times up to 48 h, and the total PanK enzyme specific activity was determined in crude cell lysates. In the DMSO-treated cells, there was no significant change in PanK enzyme activity between 0 h and 72 h of treatment (**Fig. 11**). BF treatment triggered an increase in PanK enzyme-specific activity as a function of time to a level that was approximately twice that in the control at 48 h. The PanK enzyme activity increase in response to BF was consistent with the magnitude of the observed increase in PanK1α mRNA (Fig. 5) and PanK1 protein expression (Fig. 10) levels.

BF elevated cellular CoA and P-PanSH levels

Metabolic radiolabeling of HepG2 cells with [^{3}H]Pan was performed to investigate the impact of BF-stimulated PanK expression on CoA biosynthesis. Cells were har-

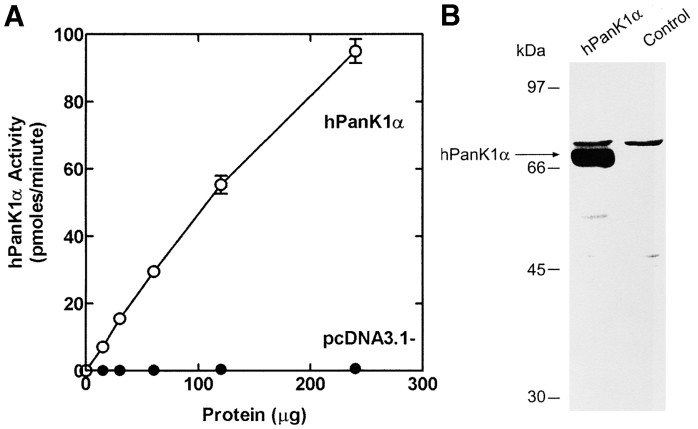

Fig. 8. hPanK1α biochemical activity. COS7 cells were transfected with either the hPanK1α cDNA expression vector or the pcDNA3.1(−) empty vector as a control. A: Pantothenate kinase (PanK) enzyme activity measured as a function of soluble lysate protein. The error bars represent duplicate data points. B: Western blot using 120 μg of lysate protein per lane and the affinity-purified PanK antibody. The enzyme assay conditions, immunoblot procedure, and antibody preparation are described under Experimental Procedures.

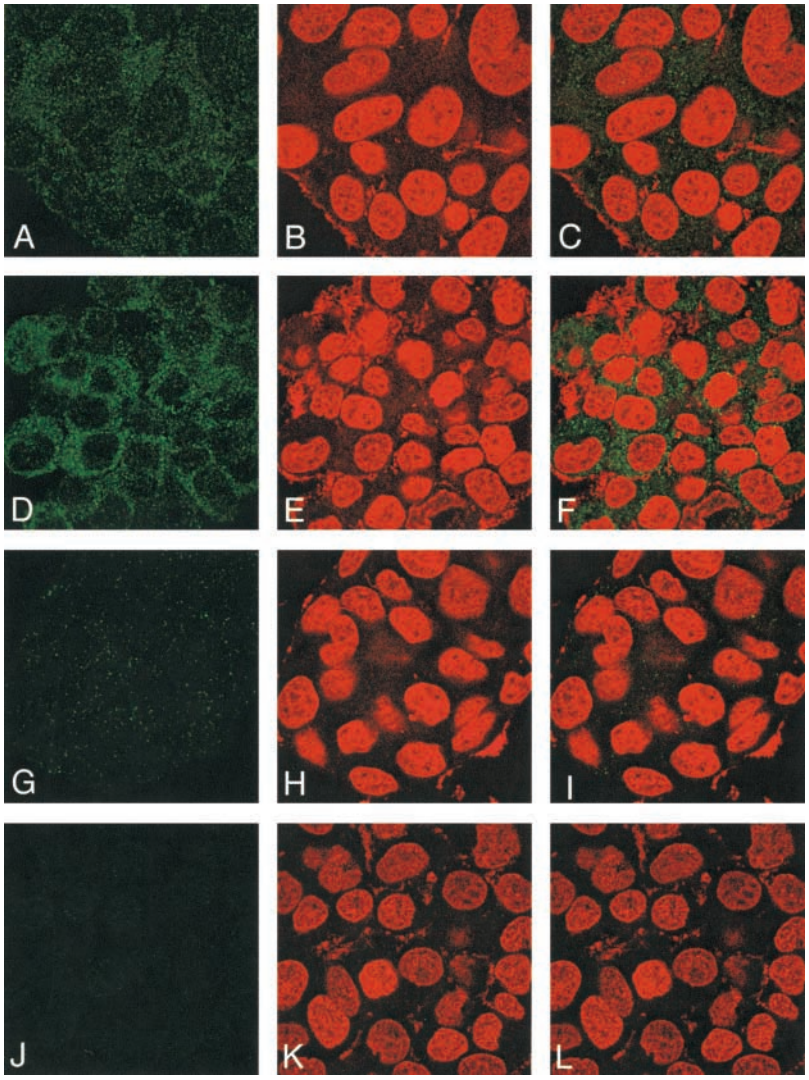

Fig. 9. Immunofluorescence/confocal images of hPanK1 protein expression in HepG2 cells. The cells were treated with DMSO (A, B, C) or 0.5 mM BF (D–L) for 72 h, and the hPanK1 protein was visualized by immunofluorescence and confocal microscopy. The panels on the left show fluorescence in the green channel (hPanK staining); panels in the middle show red fluorescence (nuclear staining); and panels on the right represent overlay images of left and middle panels. In DMSO-treated cells, cytoplasmic green fluorescence is visible (A, B, C). In BF-treated cells, there was an increase in the cytoplasmic fluorescence (D, E, F). Controls in which the primary antibody was incubated with 5-fold molar excess of the PanK antigenic epitope peptide before staining show a reduction in the cytoplasmic fluorescence intensity (G, H, I). Minimal cytoplasmic fluorescence is seen in cells stained with the secondary FITC-coupled antibody only (J, K, L). The gain settings for A–F were 605 (green) and 679 (red). For G–I, the gain settings were 594 (green) and 647 (red). The gain settings for J–L were 718 (green) and 679 (red).

vested at various times between 12 h and 72 h of BF treatment, and the soluble extract was fractionated by TLC to identify the cellular levels of CoA and various intermediates in the biosynthetic pathway. The major radiolabeled cellular pools were Pan, P-PanSH, and CoA, and these three intermediates constituted >95% of the total. There was no significant change in the total amount or ratio of phosphorylated CoA pathway intermediates in control cells between 12 h and 72 h, indicating that the radiolabeling had reached metabolic equilibrium by 12–24 h. In contrast, the phosphorylated PanK products increased after 12 h of BF treatment, reaching a maximum at 24 h that was 3.6× higher than in control cells (**Fig. 12A**), and this level was maintained up to 72 h. The amount of cellular CoA in BF-treated cells increased to a level 2.6-fold higher than that in DMSO-treated controls (Fig. 12B), and the P-PanSH increased 3.6-fold after 24 h of BF exposure (Fig. 12C). These data show that BF-stimulated PanK expression was reflected in a higher steady-state CoA level in HepG2 cells. These data are consistent with a key rate-limiting role for PanK in the CoA biosynthetic pathway, and the finding that P-PanSH also was elevated in response to BF points to the P-PanSH adenylyltransferase as a second control point in the CoA biosynthetic pathway.

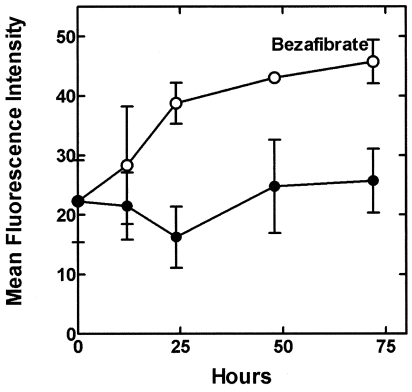

Fig. 10. Quantitation of hPanK1 protein expression. The hPanK1 protein amount was quantified for 20 cells per time point in duplicate using ImageProPlus software as described under Experimental Procedures. Mean fluorescence intensity of hPanK1 in DMSO control cells (closed circle) or in BF-treated cells (open circle) was determined using the gain settings reported in Fig. 9A–F. The error bars represent duplicate data points.

DISCUSSION

Our results point to the PPARα-mediated regulation of PanK1α expression as an important mechanism underlying the modulation of hepatic CoA levels in response to the physiological status of the animal (51). The metabolic state (starvation or feeding) (15–19), pathological conditions (diabetes) (20, 21), and hypolipidemic drugs (fibrates) (17, 22, 23) all significantly alter the cellular levels of CoA, and these fluctuations are reflected by concomitant changes in tissue PanK activity (13, 14). CoA participates in most of the reactions catalyzed by PPARα target genes (i.e., fatty acid β-oxidation), and CoA and its thioesters are also regulators of key enzymes in intermediary metabolism, such as pyruvate dehydrogenase, citrate lyase, and carnitine palmitoyl transferase. Thus, the observed adjustments in the concentration of CoA/acetyl-CoA likely contribute to the redirection of carbon flux that occurs during fasting, in diabetes, and following treatment with hypolipidemic drugs. The human *PANK1* gene structure (Fig. 1) reveals that the PanK1α and PanK1β transcripts arise from the utilization of alternate transcriptional start sites, as reported in the mouse (9). The 1β exon is removed by splicing the 1α exon to exon 2 to yield the PanK1α transcript. A survey of human tissue mRNA reveals that PanK1α expression predominates (Fig. 3), and BF stimulation of PanK expression is selective for the PanK1α isoform in the HepG2 cultured cell model (Fig. 4). The presence of four DNA sequences that correspond to PPREs in the 1α promoter region (Fig. 7A), coupled with enhanced PanK1α promoter activity in response to

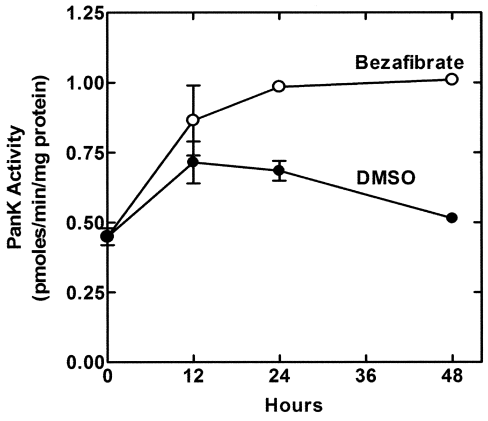

Fig. 11. BF-elevated cellular PanK-specific enzyme activity. HepG2 cells were untreated (0 h) or treated with DMSO or 0.5 mM BF for 12 h, 24 h, and 48 h. PanK enzyme activity was determined using 350 μg soluble lysate protein using the assay described under Experimental Procedures. The results represent two independent experiments performed in duplicate. The error bars represent duplicate data points.

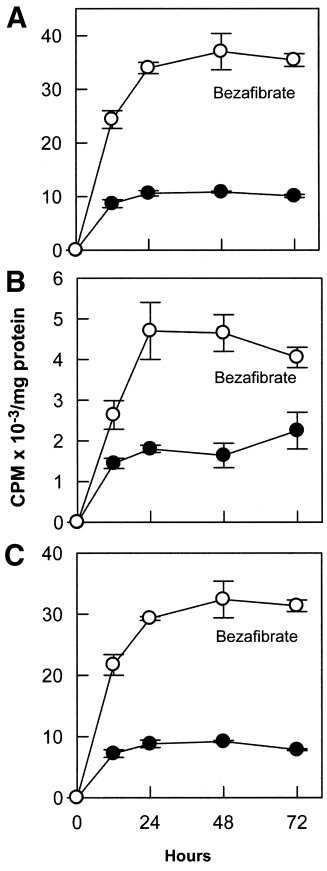

Fig. 12. BF increased intracellular CoA and 4′-phosphopantetheine (P-PanSH). HepG2 cells were labeled with D-[2,3-^{3}H]pantothenic acid (33.3 nM, specific activity 25 Ci/mmol) in pantothenate (Pan)-free DMEM in the presence of DMSO or 0.5 mM BF for 0 h, 12 h, 24 h, 48 h, and 72 h. The distribution of radiolabeled Pan metabolites was quantified in cell extracts using TLC as described under Experimental Procedures, and radioactivity was normalized to total protein in the cell extract. A: Total phosphorylated Pan metabolites in control (closed circle) and BF- (open circle) treated cells. B: CoA levels in cells treated with DMSO (closed circle) or BF (open circle). C: P-PanSH levels in control (closed circle) or BF-treated (open circle) cells. The results represent two independent experiments performed in duplicate. The error bars represent duplicate data points.

BF treatment of HepG2 cells (Fig. 7B), points to transcriptional regulation of PanK1α as a primary mechanism for the control of CoA levels by hypolipidemic agents. The elevation of PanK1α mRNA (Figs. 4, 5) leads to the concomitant increase in PanK1 protein, PanK enzyme activity, and CoA content (Figs. 10, 11, 12). The elevation of PanK1α expression and CoA content in the HepG2 model may be lower than that observed in liver, because HepG2 cells express limited amounts of PPARα protein (52). Thus, our model for CoA tissue regulation by PPARα-regulated PanK1α expression is consistent with the need to significantly increase the availability of CoA to support the accelerated processing of CoA thioesters through the β-oxidation pathway.

The biochemical analysis of allosteric PanK control (5, 8, 9, 53, 54), coupled with the genetic regulatory mechanism described in this report, points to PanK as a master switch in CoA production. Pan is usually present in excess and is rapidly taken up by cells via an active transport system (55, 56). Thus, the intracellular level of CoA is controlled by the amount of cellular PanK activity, which is a function of both the stringency of feedback regulation and the total amount of PanK protein. Feedback inhibition of PanK by CoA is a homeostatic mechanism that sets the upper limit for the intracellular CoA concentration at a given level of PanK expression (5, 8, 9, 53, 54). Feedback inhibition is critical, because in the absence of regulation, the CoA levels would depend on the dietary supply of Pan and would rise until all available Pan is converted to CoA. The level of PanK expression establishes the intracellular level of CoA by changing the set point established by feedback regulation. Increased expression of PanK will cause the CoA/CoA thioester pool to expand until it reaches a new steady-state level that effectively switches off the flux through the pathway via the feedback inhibition loop. The fact that mammalian PanK isoforms have different sensitivities to feedback regulation (9) illustrates that CoA levels will change by different degrees, depending not only on the amount of PanK expressed but also on which isoform is being genetically regulated. The accumulation of P-PanSH following increased PanK expression (Fig. 12) (8) indicates that P-PanSH adenylyltranferase, CoA phosphodiesterase, and/or organelle-specific transport systems (see below) are a second site for controlling total CoA content. This secondary regulatory point has been observed before using plasmid-driven overexpression of both the bacterial PanK protein (57) and the mouse PanK1β (8). Bacterial P-PanSH adenylyltransferase is likely feedback inhibited by CoA (58), but this property has not been explored in the related mammalian multifunctional CoA synthase.

The compartmentation of the CoA biosynthetic pathway is of considerable interest, because the highest concentrations of CoA exist in organelles. In general, cytosolic concentrations of CoA are estimated at between 0.02 and 0.06 mM, whereas mitochondrial concentrations range from 2.2 to 2.6 mM (59, 60). Peroxisomes also have high concentrations of CoA (61, 62). The requirement for high levels of CoA in peroxisomes is consistent with the increases in CoA biosynthesis and tissue CoA levels following treatment with peroxisome proliferators (17). The observation that fibrates do not elicit their hypolipidemic effects in PAN-deficient animals (63) illustrates that accelerated CoA production is essential to the biogenesis of functional peroxisomes. Our model for CoA elevation via PPARα-stimulated PanK1α expression (22, 23) provides a mechanism for the boosting of CoA biosynthesis to supply the growing CoA demand of the expanding peroxisomal compartment. Our work indicates that hPanK1 is a cytosolic protein (Fig. 9), and sequence analysis did not reveal the presence of known peroxisome targeting signals. These data suggest either that intact CoA is transported into peroxisomes or that peroxisomes contain a CoA synthase (P-PanSH adenylyltransferase/dephosphoCoA kinase) and import P-PanSH from the cytosol. Recently, a CoA hydrolase was identified in peroxisomes (64, 65), which provides a mechanism for this organelle to decrease the CoA concentration. Clearly, the regulation of organelle CoA content is complex and likely governed by the interplay among CoA biosynthesis, transport, and degradation.

The importance of CoA compartmentation is highlighted by the recent discovery that Hallervorden-Spatz syndrome (HSS), an autosomal recessive neurodegenerative disorder (66), likely arises from dysregulated mitochondrial CoA metabolism. The disorder is associated with the deposition of iron in the basal ganglia (67) and serves as a model for complex neurodegenerative diseases, such as Parkinson's disease (68), Alzheimer's disease (69), and Huntington's disease (70), which, like HSS, all exhibit pathologic accumulation of iron in the brain. Mutations that inactivate one isoform of human PanK, *PANK2*, are the causative agent of HSS, and the disease was renamed PanK-associated neurodegeneration (10). The similarity of the pathology of PKAN to that of the disorders listed above led Zhou et al. (10) to suggest that perturbed Pan metabolism may be a general feature of neurodegenerative diseases. Importantly, one of the isoforms encoded by the *PANK2* gene localizes to mitochondria (11). This discovery suggests that mitochondria may have the entire complement of CoA biosynthetic enzymes. Previous work hypothesized that mitochondrial CoA arises either from P-PanSH transport followed by conversion to CoA by a mitochondrial form of the bifunctional CoA synthase (71, 72) or from the presence of a mitochondrial CoA transporter (73–75). Thus, organelles may possess multiple mechanisms for increasing their CoA content that would allow PPARα-stimulated cytosolic PanK1α to provide additional CoA for mitochondrial metabolism via one of the transport mechanisms, while the steady-state mitochondrial CoA level is governed by the constitutive expression of the PanK2 isoform.

The authors thank Pam Jackson for expert molecular biology, and Chuck Rock for helpful discussion and comments on the manuscript. This work was supported by National Institutes of Health Grant GM-62896 (S.J.), Cancer Center (CORE) support grant CA21765, and the American and Lebanese Syrian Associated Charities.

REFERENCES

1. Abiko, Y. 1975. Metabolism of coenzyme A. *In* Metabolic Pathways. D. M. Greenburg, editor. Academic Press, Inc., New York. 1–25.
2. Jackowski, S. 1996. Biosynthesis of pantothenic acid and coenzyme A. *In Escherichia coli* and *Salmonella typhimurium*: Cellular and Molecular Biology. F. C. Neidhardt, R. Curtiss, C. A. Gross, J. L. Ingraham, E. C. C. Lin, K. B. Low, B. Magasanik, W. Reznikoff, M. Riley, M. Schaechter, and H. E. Umbarger, editors. American Society for Microbiology, Washington, D.C. 687–694.
3. Robishaw, J. D., and J. R. Neely. 1985. Coenzyme A metabolism. *Am. J. Physiol.* **248:** E1–E9.
4. Daugherty, M., B. Polanuyer, M. Farrell, M. Scholle, A. Lykidis, V. Crecy-Lagard, and A. Osterman. 2002. Complete reconstitution of the human coenzyme A biosynthetic pathway via comparative genomics. *J. Biol. Chem.* **277:** 21431–21439.
5. Vallari, D. S., S. Jackowski, and C. O. Rock. 1987. Regulation of pantothenate kinase by coenzyme A and its thioesters. *J. Biol. Chem.* **262:** 2468–2471.
6. Jackowski, S., and C. O. Rock. 1981. Regulation of coenzyme A biosynthesis. *J. Bacteriol.* **148:** 926–932.
7. Robishaw, J. D., D. A. Berkich, and J. R. Neely. 1982. Rate-limiting step and control of coenzyme A synthesis in cardiac muscle. *J. Biol. Chem.* **257:** 10967–10972.
8. Rock, C. O., R. B. Calder, M. A. Karim, and S. Jackowski. 2000. Pantothenate kinase regulation of the intracellular concentration of coenzyme A. *J. Biol. Chem.* **275:** 1377–1383.
9. Rock, C. O., M. A. Karim, Y-M. Zhang, and S. Jackowski. 2002. The murine *Pank1* gene encodes two differentially regulated pantothenate kinase isozymes. *Gene.* **291:** 35–43.
10. Zhou, B., S. K. Westaway, B. Levinson, M. A. Johnson, J. Gitschier, and S. J. Hayflick. 2001. A novel pantothenate kinase gene (*PANK2*) is defective in Hallervorden-Spatz syndrome. *Nat. Genet.* **28:** 345–349.
11. Hortnagel, K., H. Prokisch, and T. Meitinger. 2003. An isoform of hPANK2, deficient in pantothenate kinase-associated neurodegeneration, localizes to mitochondria. *Hum. Mol. Genet.* **12:** 321–327.
12. Ching, K. H., S. K. Westaway, J. Gitschier, J. J. Higgins, and S. J. Hayflick. 2002. HARP syndrome is allelic with pantothenate kinase-associated neurodegeneration. *Neurology.* **58:** 1673–1674.
13. Halvorsen, O. 1983. Effects of hypolipidemic drugs on hepatic CoA. *Biochem. Pharmacol.* **32:** 1126–1128.
14. Skrede, S., and O. Halvorsen. 1979. Increased biosynthesis of CoA in the liver of rats treated with clofibrate. *Eur. J. Biochem.* **98:** 223–229.
15. Kondrup, J., and N. Grunnet. 1973. The effect of acute and prolonged ethanol treatment on the contents of coenzyme A, carnitine and their derivatives in rat liver. *Biochem. J.* **132:** 373–379.
16. Lund, H., J. A. Stakkestad, and S. Skrede. 1986. Effects of thyroid state and fasting on the concentrations of CoA and malonyl-CoA in rat liver. *Biochim. Biophys. Acta.* **876:** 685–687.
17. Savolainen, M. J., V. P. Jauhonen, and I. E. Hassinen. 1977. Effects of clofibrate on ethanol-induced modifications in liver and adipose tissue metabolism: role of hepatic redox state and hormonal mechanisms. *Biochem. Pharmacol.* **26:** 425–431.
18. Smith, C. M., M. L. Cano, and J. Potyraj. 1978. The relationship between metabolic state and total CoA content of rat liver and heart. *J. Nutr.* **108:** 854–862.
19. Smith, C. M., and C. R. Savage, Jr. 1980. Regulation of coenzyme A biosynthesis by glucagon and glucocorticoid in adult rat liver parenchymal cells. *Biochem. J.* **188:** 175–184.
20. Reibel, D. K., B. W. Wyse, D. A. Berkich, W. M. Palko, and J. R. Neely. 1981. Effects of diabetes and fasting on pantothenic acid metabolism in rats. *Am. J. Physiol.* **240:** E597–E601.
21. Reibel, D. K., B. W. Wyse, D. A. Berkich, and J. R. Neely. 1981. Regulation of coenzyme A synthesis in heart muscle: effects of diabetes and fasting. *Am. J. Physiol.* **240:** H606–H611.
22. Bhuiyan, A. K. M. J., K. Bartlett, H. S. A. Sherratt, and L. Agius. 1988. Effects of ciprofibrate and 2-[5-(4-chlorophenyl)pentyl]oxirane-2-carboxylate (POCA) on the distribution of carnitine and CoA and their acyl-esters and on enzyme activities in rats. *Biochem. J.* **253:** 337–343.
23. Voltti, H., M. J. Savolainen, V. P. Jauhonen, and I. E. Hassinen. 1979. Clofibrate-induced increase in coenzyme A concentration in rat tissues. *Biochem. J.* **182:** 95–102.
24. Schoonjans, K., B. Staels, and J. Auwerx. 1996. The peroxisome proliferator activated receptors (PPARS) and their effects on lipid metabolism and adipocyte differentiation. *Biochim. Biophys. Acta.* **1302:** 93–109.
25. Green, S. 1995. PPAR: a mediator of peroxisome proliferator action. *Mutat. Res.* **333:** 101–109.
26. Schoonjans, K., B. Staels, and J. Auwerx. 1996. Role of the peroxisome proliferator-activated receptor (PPAR) in mediating the effects of fibrates and fatty acids on gene expression. *J. Lipid Res.* **37:** 907–925.
27. Gulick, T., S. Cresci, T. Caira, D. D. Moore, and D. P. Kelly. 1994. The peroxisome proliferator-activated receptor regulates mitochondrial fatty acid oxidative enzyme gene expression. *Proc. Natl. Acad. Sci. USA.* **91:** 11012–11016.
28. Tugwood, J. D., I. Issemann, R. G. Anderson, K. R. Bundell, W. L. McPheat, and S. Green. 1992. The mouse peroxisome proliferator activated receptor recognizes a response element in the 5′ flanking sequence of the rat acyl CoA oxidase gene. *EMBO J.* **11:** 433–439.
29. Kliewer, S. A., K. Umesono, D. J. Noonan, R. A. Heyman, and R. M. Evans. 1992. Convergence of 9-cis retinoic acid and peroxisome proliferator signalling pathways through heterodimer formation of their receptors. *Nature.* **358:** 771–774.
30. Ni, X., Y. Ma, H. Cheng, M. Jiang, K. Ying, Y. Xie, and Y. Mao. 2002. Cloning and characterization of a novel human pantothenate kinase gene. *Int. J. Biochem. Cell Biol.* **34:** 109–115.
31. Karim, M. A., V. A. Valentine, and S. Jackowski. 2000. Human pantothenate kinase 1 (PANK1) gene: characterization of the cDNAs, structural organization and mapping of the locus to chromosome 10q23.2–23.31 (Abstract). *Am. J. Hum. Genet.* **67:** 185.
32. Kingston, R. E. 1998. CsCl purification of RNA from cultured cells. *In* Current Protocols in Molecular Biology. F. M. Ausubel, R. Brent, R. E. Kingston, D. D. Moore, J. G. Seidman, J. A. Smith, and K. Struhl, editors. John Wiley & Sons, New York. 4.2.3–4.2.9.
33. Bradford, M. M. 1976. A rapid and sensitive method for quantitation of microgram quantities of protein utilizing the principle of protein-dye binding. *Anal. Biochem.* **72:** 248–254.
34. Johnson, G. D., and G. M. C. Araujo. 1981. A simple method of reducing the fading of immunofluorescence during microscopy. *J. Immunol. Methods.* **43:** 349–350.
35. Vigneri, P., and J. Y. J. Wang. 2001. Induction of apoptosis in chronic myelogenous leukemia cells through nuclear entrapment of BCR-ABL tyrosine kinase. *Nat. Med.* **7:** 228–234.
36. Wolfrum, C., C. Buhlmann, B. Rolf, T. Borchers, and F. Spener. 1999. Variation of liver-type fatty acid binding protein content in the human hepatoma cell line HepG2 by peroxisome proliferators and antisense RNA affects the rate of fatty acid uptake. *Biochim. Biophys. Acta.* **1437:** 194–201.
37. Miller, D. B., and J. D. Spence. 1998. Clinical pharmacokinetics of fibric acid derivatives (fibrates). *Clin. Pharmacokinet.* **34:** 155–162.
38. Wolfrum, C., P. Ellinghaus, M. Fobker, U. Seedorf, G. Assmann, T. Borchers, and F. Spener. 1999. Phytanic acid is ligand and transcriptional activator of murine liver fatty acid binding protein. *J. Lipid Res.* **40:** 708–714.
39. Lekas, P., K. L. Tin, and R. D. Prokipcak. 2000. The human cytochrome P4501A1 mRNA is rapidly degraded in HepG2 cells. *Arch. Biochem. Biophys.* **384:** 311–318.
40. Prokipcak, R. D., A. Raouf, and C. Lee. 2000. The AU-rich 3′ untranslated region of human MDR1 mRNA is an inefficient mRNA destabilizer. *Arch. Biochem. Biophys.* **261:** 627–634.
41. Baumann, C. A., N. Chokshi, A. R. Saltiel, and V. Ribon. 2000. Cloning and characterization of a functional peroxisome proliferator activator receptor-γ-responsive element in the promoter of the *CAP* gene. *J. Biol. Chem.* **275:** 9131–9135.
42. Heinemeyer, T., E. Wingender, I. Reuter, H. Hermjakob, A. E. Kel, O. V. Kel, E. V. Ignatieva, E. A. Ananko, O. A. Podkolodnaya, F. A. Kolpakov, N. L. Podkolondnaya, and N. A. Kolchanov. 1998. Databases on transcriptional regulation: TRANSFAC, TRRD, and COMPEL. *Nucleic Acids Res.* **26:** 364–370.
43. Koo, S. H., and H. C. Towle. 2000. Glucose regulation of mouse S14 gene expression in hepatocytes. *J. Biol. Chem.* **275:** 5200–5207.
44. Kawaguchi, R., K. Osatomi, H. Yamashita, T. Kabashima, and K. Uyeda. 2002. Mechanism for fatty acid 'spareing' effect on glucose-induced transcription. *J. Biol. Chem.* **277:** 3829–3835.
45. Shih, H. M., Z. Liu, and H. C. Towle. 1995. Two CACGTG motifs with proper spacing dictate the carbohydrate regulation of hepatic gene transcription. *J. Biol. Chem.* **270:** 21991–21997.
46. Wang, H., and C. B. Wollheim. 2002. ChREBP rather than USF2

regulates glucose stimulation of endogenous L-pyruvate kinase expression in insulin-secreting cells. *J. Biol. Chem.* **277:** 32746–32752.
47. Yahagi, N., H. Shimano, A. H. Hasty, T. Matsuzaka, T. Ide, T. Yoshikawa, M. Amemiya-Kudo, S. Tomita, H. Okazaki, Y. Tamura, Y. Iizuka, K. Ohashi, J. J. Osuga, K. Harada, T. Gotoda, R. Nagai, S. Ishibashi, and N. Yamada. 2002. Absence of sterol regulatory element-binding protein-1 (SREBP-1) ameliorates fatty livers but not obesity or insulin resistance in Lep(ob)/Lep(ob) mice. *J. Biol. Chem.* **277:** 19353–19357.
48. Sun, L., N. Halaihel, W. Zhang, T. Roger, and M. Levi. 2002. Role of sterol regulatory element-binding protein 1 in regulation of renal lipid metabolism and glomerulosclerosis in diabetes mellitus. *J. Biol. Chem.* **277:** 18919–18927.
49. Torra, I. P., Y. Jamshidi, D. M. Flavell, J-C. Fruchart, and B. Staels. 2002. Characterizatgion of the human PPARα promoter: identification of a functional nuclear receptor response element. *Mol. Endocrinol.* **16:** 1013–1028.
50. Roduit, R., J. Morin, F. Masse, L. Segall, E. Roche, C. B. Newgard, F. Assimacopoulos-Jeannet, and M. Prentki. 2000. Glucose downregulates the expression of the peroxisome proliferator-activated receptor-alpha gene in the pancreatic beta cell. *J. Biol. Chem.* **275:** 35799–35806.
51. Tahiliani, A. G., and C. J. Beinlich. 1991. Pantothenic acid in health and disease. *Vitam. Horm.* **46:** 165–228.
52. Hsu, M. H., U. Savas, K. J. Griffin, and E. F. Johnson. 2001. Identification of peroxisome proliferator-responsive human genes by elevated expression of the peroxisome proliferator-activated receptor α in HepG2 cells. *J. Biol. Chem.* **276:** 27950–27958.
53. Rock, C. O., H-W. Park, and S. Jackowski. 2003. Role of feedback regulation of pantothenate kinase (CoaA) in the control of coenzyme A levels in *Escherichia coli*. *J. Bacteriol.* **185:** 3410–3415.
54. Calder, R. B., R. S. B. Williams, G. Ramaswamy, C. O. Rock, E. Campbell, S. E. Unkles, J. R. Kinghorn, and S. Jackowski. 1999. Cloning and characterization of a eukaryotic pantothenate kinase gene (*panK*) from *Aspergillus nidulans*. *J. Biol. Chem.* **274:** 2014–2020.
55. Vallari, D. S., and C. O. Rock. 1985. Pantothenate transport in *Escherichia coli*. *J. Bacteriol.* **162:** 1156–1161.
56. Barbarat, B., and R. A. Podevin. 1986. Pantothenate-sodium cotransport in renal brush-border membranes. *J. Biol. Chem.* **261:** 14455–14460.
57. Song, W-J., and S. Jackowski. 1992. Cloning, sequencing, and expression of the pantothenate kinase (*coaA*) gene of *Escherichia coli*. *J. Bacteriol.* **174:** 6411–6417.
58. Geerlof, A., A. Lewendon, and W. V. Shaw. 1999. Purification and characterization of phosphopantetheine adenylyltransferase from *Escherichia coli*. *J. Biol. Chem.* **274:** 27105–27111.
59. Idell-Wenger, J., L. Grotyohann, and J. R. Neely. 1978. Coenzyme A and carnitine distribution in normal and ischemic hearts. *J. Biol. Chem.* **253:** 4310–4318.
60. Williamson, J., and B. Corkey. 1979. Assay of citric acid cycle intermediates and related compounds—uptake with tissue metabolite levels and intracellular distribution. *Methods Enzymol.* **55:** 200–222.
61. Horie, S., M. Isobe, and T. Suga. 1986. Changes in CoA pools in hepatic peroxisomes of the rat under various conditions. *J. Biochem.* **99:** 1345–1352.
62. Van Broekhoven, A., M-C. Peeters, L. J. Debeer, and G. P. Mannaerts. 1981. Subcellular distribution of coenzyme A: evidence for a separate coenzyme A pool in peroxisomes. *Biochem. Biophys. Res. Commun.* **100:** 305–312.
63. Youssef, J. A., W. O. Song, and M. Z. Badr. 1997. Mitochondrial, but not peroxisomal, β-oxidation of fatty acids is conserved in coenzyme A-deficient rat liver. *Mol. Cell. Biochem.* **175:** 37–42.
64. Cartwright, J. L., L. Gasmi, D. G. Spiller, and A. G. McLennan. 2000. The *Saccharomyces cerevisiae* PCD1 gene encodes a peroxisomal nudix hydrolase active toward coenzyme A and its derivatives. *J. Biol. Chem.* **275:** 32925–32930.
65. Gasmi, L., and A. G. McLennan. 2001. The mouse *Nudt7* gene encodes a peroxisomal nudix hydrolase specific for coenzyme A and its derivatives. *Biochem. J.* **357:** 33–38.
66. Dooling, E. C., W. C. Schoene, and E. P. Richardson, Jr. 1974. Hallervorden-Spatz syndrome. *Arch. Neurol.* **30:** 70–83.
67. Swaiman, K. F. 1991. Hallervorden-Spatz syndrome and brain iron metabolism. *Arch. Neurol.* **48:** 1285–1293.
68. Sofic, E., P. Riederer, H. Heinsen, H. Beckmann, G. P. Reynolds, G. Hebenstreit, and M. B. Youdim. 1988. Increased iron (III) and total iron content in post mortem substantia nigra of parkinsonian brain. *J. Neural Transm.* **74:** 199–205.
69. Connor, J. R., B. S. Snyder, J. L. Beard, R. E. Fine, and E. J. Mufson. 1992. Regional distribution of iron and iron-regulatory proteins in the brain in aging and Alzheimer's disease. *J. Neurosci. Res.* **31:** 327–335.
70. Dexter, D. T., A. Carayon, F. Javoy-Agid, Y. Agid, F. R. Wells, S. E. Daniel, A. J. Lees, P. Jenner, and C. D. Marsden. 1991. Alterations in the levels of iron, ferritin and other trace metals in Parkinson's disease and other neurodegenerative diseases affecting the basal ganglia. *Brain.* **114:** 1953–1975.
71. Worrall, D. M., and P. K. Tubbs. 1983. A bifunctional enzyme complex in coenzyme A biosynthesis: purification of 4′ pantetheine phosphate adenylyltransferase and dephospho-CoA kinase. *J. Biochem. (Tokyo).* **215:** 153–157.
72. Skrede, S., and O. Halvorsen. 1983. Mitochondrial pantetheinephosphate adenylytransferase and dephospho-CoA kinase. *Eur. J. Biochem.* **131:** 57–63.
73. Tahiliani, A. G., and J. R. Neely. 1987. A transport system for coenzyme A in isolated rat heart mitochondria. *J. Biol. Chem.* **262:** 11607–11610.
74. Tahiliani, A. G. 1989. Dependence of mitochondrial coenzyme A uptake on the membrane electrical gradient. *J. Biol. Chem.* **264:** 18426–18432.
75. Neuburger, M., D. A. Day, and R. Douce. 1984. Transport of coenzyme A in plant mitochondria. *Arch. Biochem. Biophys.* **229:** 253–258.